ChemPubSoc Europe

DOI: 10.1002/cphc.201300602

Difference in the Photophysical Properties of a Perylenetetracarboxylic Diimide Dimer and a Hexamer Linked by the Same Hexaphenylbenzene Group

Lin Xue, Yan Shi, Liangliang Zhang, and Xiyou Li*[a]

A perylenetetracarboxylic diimide hexamer (6PDI) and a dimer (2PDI) linked with the same hexaphenylbenzene group were prepared, and the structures were fully characterized by ^{1}H NMR spectroscopy, mass spectrometry, and elemental analysis. Due to the similar molecular structure of these two compounds, similar interactions between/among the PDI subunits as well as similar photophysical properties are expected. However, the stationary UV/Vis absorption spectra reveal that the interactions among/between the PDI subunits in 6PDI are significantly stronger than those in 2PDI. This can be attributed to blocked rotation along the long axis of the PDI subunits in 6PDI due to steric hindrance of the two neighboring PDI subunits. The stronger interactions among the PDI subunits in 6PDI lead to long-wavelength emission, which can be assigned to "excimer-like" excited states. A similar conclusion can also be deduced from the fluorescence quantum yields and the fluorescence lifetimes. Electrochemical studies revealed that interactions between/among the PDI subunits in both 2PDI and 6PDI are still in the range of weak interactions. Ultrafast transient anisotropy decay dynamics revealed that excitation delocalization between the PDI subunits within 2PDI and 6PDI is quick and efficient. More interestingly, delocalization is faster in 6PDI than in 2PDI, probably because of the stronger interactions among the PDI subunits in the former.

1. Introduction

In the bacterial photosynthetic antenna of light-harvesting complexes 1 and 2 (LH1 and LH2), photosynthetic tetrapyrrolic pigments are deliberately positioned in a wheel-like arrangement.[1–3] The absorbed light energy is transferred through intra- or interwheel excitation energy transfer (EET) to the reaction center. Inspired by these perfect architectures, cyclic and dendritic molecular arrays of organic dyes have been explored, and intramolecular EET has been studied with the goal of applying these molecular arrays to molecular photonic devices or artificial light-harvesting systems.[4–9] The most popular organic dyes investigated in this field are porphyrins because their molecular structures and photophysical properties are similar to those of natural bacteriochlorophyll *a* (Bchl *a*).[10–23] However, the use of light-harvesting systems in molecular photonic devices requires different types of molecular arrays with different properties. Therefore, molecular arrays of organic dyes other than porphyrin were also developed in the past several decades.[24–30] Among the numerous organic dyes employed in artificial light-harvesting studies, perylenentetracarboxylic diimide (PDI) compounds play an important role, because of their excellent stability towards heat and light as well as their high fluorescence quantum yields (almost 100%) and large extinction coefficients in the visible-light region.[31–38] Most importantly, PDI molecules can be easily modified and decorated at the imide nitrogen atoms or the peripheral positions, and thus, their properties can be conventionally tuned to meet the needs of different applications.[39,40]

In these numerous PDI-based molecular arrays, one group of compounds, which are composed of several PDI subunits with precisely controlled relative orientations, are designed and prepared with the goal of revealing the effects of molecular interactions between the PDI subunits on their photophysical properties. For instance, Wasielewski and co-workers reported a PDI dimer linked by a xanthene spacer[41] that showed a blueshifted band in its absorption spectrum and excimer emission in the long-wavelength region in its fluorescence spectrum. Similar properties were also presented by PDI dimers with flexible linkages.[42,43] The photophysical properties of these dimeric PDIs can be explained as the result of the interaction between two transitions that occur parallel to each according to exciton theory. A more rigid structure of the PDI dimers results in higher emission efficiency of the excimer as well as a longer fluorescence lifetime.[44] Decorating the PDI rings with electron-donating amino groups at the bay positions in a PDI dimer leads to significant quenching of the emission of the excimer. A charge-separated state is observed for this PDI dimer, which is similar with that found for the special pair in natural photosynthesis.[45] PDI trimers with face-to-face stacked structures were also reported recently by Wasielewski and co-workers.[46,47] The corresponding lowest excited singlet states of the PDI trimers are dimerlike in nature, and this suggests that

[a] L. Xue,[+] Y. Shi,[+] L. Zhang, Prof. X. Li
Key Laboratory of Colloid and Interface Chemistry, Ministry of Education of China, Department of Chemistry, Shandong University
Shanda nan lu, #27, Jinan, Shandong, 250100 (China)
Fax: (+86) 531-88564464
E-mail: xiyouli@sdu.edu.cn

[+] These authors contributed equally to this work.

Supporting information for this article is available on the WWW under http://dx.doi.org/10.1002/cphc.201300602.

WILEY ONLINE LIBRARY © 2013 Wiley-VCH Verlag GmbH & Co. KGaA, Weinheim

structural distortions that accompany the formation of the trimers are sufficient to confine the electronic interaction within two chromophores of these systems. Some PDI arrays with relatively weak interactions between/among the PDI subunits were also reported. Matak and co-workers reported a PDI hexamer linked by a hexaazatriphenylene group that shows a tendency to undergo aggregation due to strong π–π interactions between the molecules. No significant changes in the photophysical properties of the hexamer were identified in comparison with those of the monomer because of the large distances between the PDI subunits.[48] A similar phenomenon was also reported for a PDI trimer.[49] A perylenemonocarboxylic imide (PMI) hexamer linked with a hexaperihexabenzocoronene (HBC) group was reported by Müllen. Intramolecular energy or electron transfer between HBC and PMI was revealed by steady-state absorption and fluorescence spectroscopy.[50] A PDI hexamer linked with HBC was found to form different aggregates in solution as well as in solid films. The different aggregation behavior of HBC and PDI leads to different photoinduced processes.[51] More interestingly, molecular arrays of PDI with relative orthogonal orientations have also been reported. Although the ground-state interactions between the PDI subunits are weak due to the relative orthogonal orientation of neighboring transitions, energy transfer can occur with high efficiency and a high rate constant.[52,53] Some flexible PDI arrays can also be found in the literature. Because the flexible structure brings more complicated interactions between the neighboring PDI subunits, reliable structure–property relationships cannot be established in these molecules.[54,55] In summary, some primary relationships between the structures and the photophysical properties of the PDI arrays have been established, but they are far from being fully understood. To promote the use of PDI arrays as antenna systems in artificial photosynthesis, further detailed studies on structure–property relationships are necessary.

In the present work, we designed a covalently linked PDI hexamer with a hexaphenylbenzene group as a linkage (i.e. 6PDI, Scheme 1). For the sake of comparison, a dimer linked with same linkage at the *ortho* positions was also prepared, that is, 2PDI. The most important characteristic of these two molecules is that the relative orientation of the neighboring PDI molecules is neither parallel nor orthogonal; instead, the PDI molecules form a dihedral angle of 60°. Another important feature is the wheel-like structure of the hexamer, which mimics the B850 cycle in LH2. With these two compounds, we can estimate the effects of the relative orientation and the wheel structure on the migration of the excitation energy in these molecules.

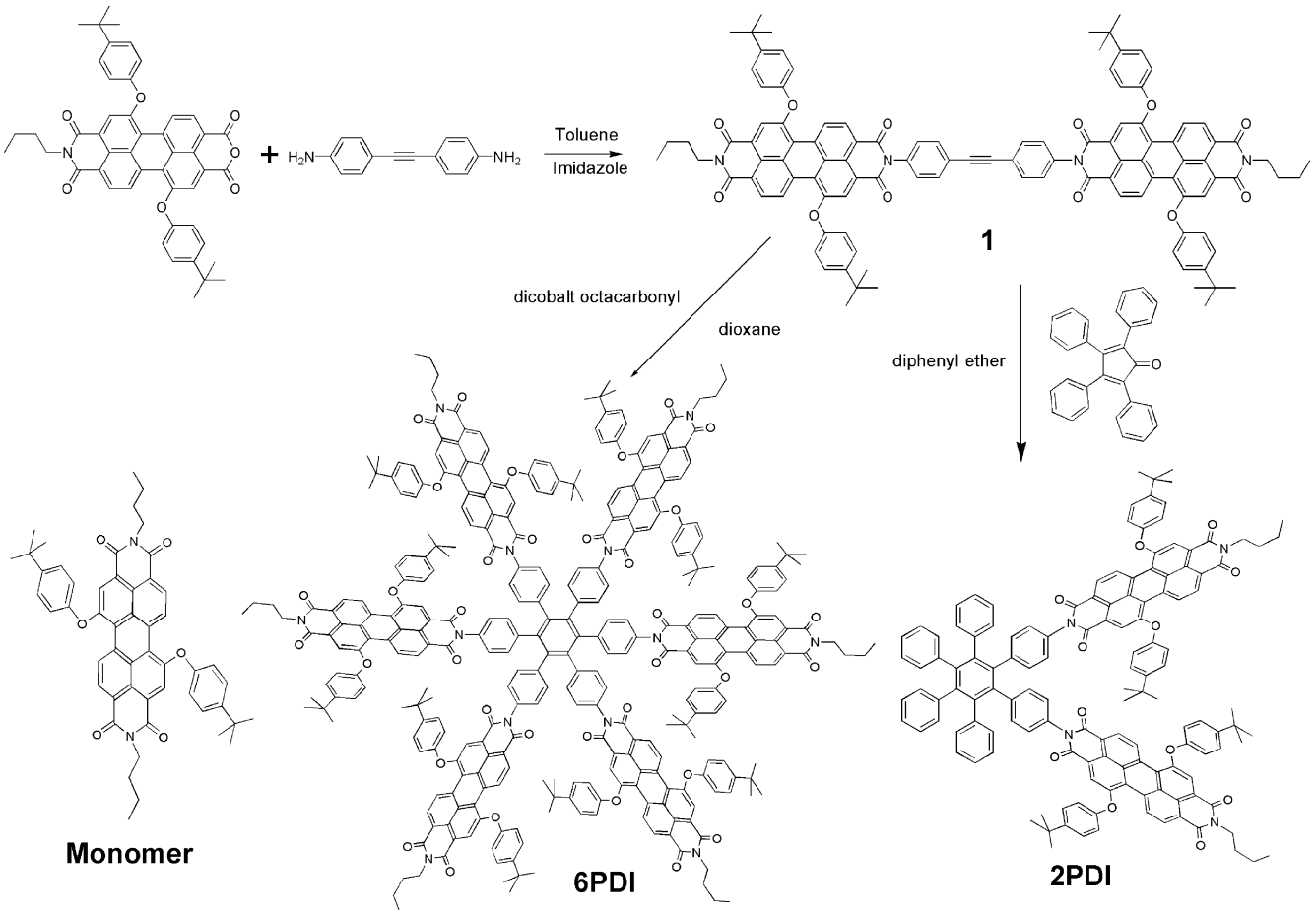

Scheme 1. Synthesis of the monomer, 2PDI, and 6PDI

© 2013 Wiley-VCH Verlag GmbH & Co. KGaA, Weinheim

2. Results and Discussion

Molecular Design and Synthesis

The linkage we chose for these two compounds is a popular building block for similar compounds such as the porphyrin hexamer[56] and ferrocene hexamer.[57] The synthesis is shown in Scheme 1. Intermediate **1** was prepared by the reaction of 1,7-di(4-*tert*-butylphenoxyl)-*N*-butyl-perylene-3,4-dicarboxylic imide-9,10-dicarboxylic anhydride with di(4-aminophenyl)ethyne[58] in reasonable yield. 2PDI was prepared by the reaction of **1** with tetraphenylcyclopentadienone in diphenyl ether under an atmosphere of nitrogen. 6PDI was prepared by the trimerization of **1** in refluxing 1,4-dioxane with $Co_2(CO)_8$ as the catalyst. To prevent the influence of air, the catalytic reaction was performed in a glove box. The product was purified by column chromatography on silica gel first and then further purified by preparative thin-layer chromatography on silica gel. The product gave a correct MALDI-TOF mass spectrum and elemental analysis results. However, its ^{1}H NMR spectrum shows only broad peaks without any fine structure. This is because 6PDI is actually a mixture of isomers, which results from hindered free rotation of the single bond between the imide nitrogen atom and the carbon atom of the phenyl ring due to steric hindrance. Because the phenoxy groups at the 1,7-positions of the perylene core are not symmetrically connected, hindered rotation results in many isomers of 6PDI. All of the other new compounds were fully characterized by ^{1}H NMR spectroscopy, MALDI-TOF mass spectrometry, and elemental analysis.

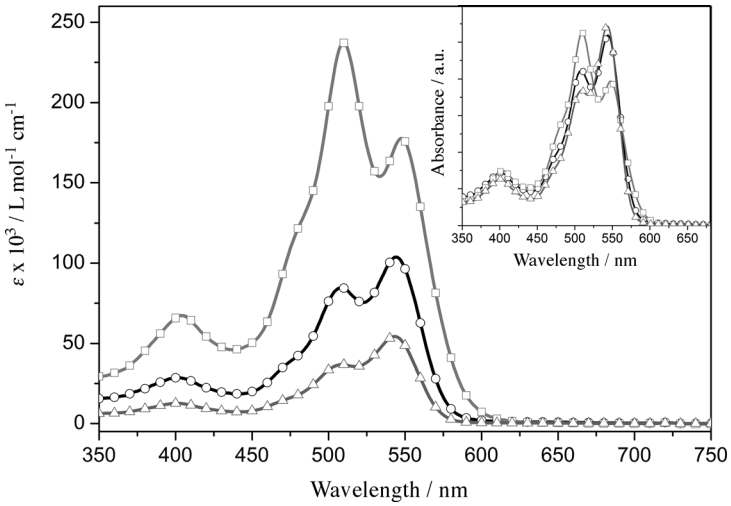

Figure 1. Absorption spectra of 6PDI (□), 2PDI (○), and the monomer (△) in CH_2Cl_2 (1×10^{-6} mol L^{-1}). The inset shows the normalized (at 541 nm) absorption spectra of the monomer, 2PDI, and 6PDI.

Table 1. Parameters of the absorption and fluorescence spectra of the monomer, 2PDI, and 6PDI.

Compound	λ_{abs} [nm] ($\varepsilon\times10^4$ [mol^{-1} L cm^{-1}])	λ_f [nm]	Φ_f[a]	τ_f [ns] (%)[b]
monomer	543 (5.44), 509(3.59)	575	1.0	4.5 (100)
2PDI	544 (10.4), 509(7.90)	578	0.42	4.3(85), 6.7 (15)
6PDI	544 (24.2), 509(19.6)	588	0.08	4.1(72), 8.3 (28)

[a] With monomer as a reference ($\Phi_f = 1$). [b] The lifetimes were measured for fluorescence at 600 nm.

Absorption and Fluorescence Spectra

UV/Vis absorption spectroscopy is sensitive to interchromophore distances and orientation, and thus it has been widely used to evaluate inter- and intramolecular interactions between large π systems.[59,60] The absorption spectra of 2PDI, 6PDI, and the monomer are shown in Figure 1, and the corresponding spectral parameters are summarized in Table 1. Two absorption peaks at about 545 and 510 nm are observed in the absorption spectra of both 2PDI and 6PDI, and this is similar that observed for the monomer. The two absorption bands can be assigned to the 0–0 and 0–1 vibration bands of the S_0–S_1 transition, respectively. Although there is no clear difference in the wavelengths of the bands in the absorption spectra of 2PDI, 6PDI, and the monomer, the intensity ratio of the 0–0 and 0–1 bands clearly changes as the number of the PDI subunits in one molecule increases. For the monomer, the intensity of the 0–1 vibration band is very small, but in the spectrum of 2PDI, the relative intensity is clearly increased, and in the spectrum of 6PDI, the intensity is increased even further. These changes in the absorption spectra suggest the presence of ground-state interactions between the PDI subunits in both 2PDI and 6PDI. Following a previous report, the 0–0 and 0–1 transitions should reverse in intensity upon π–π stacking, and the intensity of the bands at 510 and 545 nm can be directly correlated to the ratio of aggregates to the monomer in solution as well as to the strength of the interactions between the PDI subunits.[51,61] On the basis of the molecular structure shown in Scheme 1, the relative orientation of the PDI subunits in 2PDI and 6PDI is the same and interactions between them should also be theoretically identical. The difference between the absorption spectra of 2PDI and 6PDI may result from intermolecular aggregation of 6PDI. To verify this point, we recorded the temperature-dependent and concentration-dependent absorption spectra of 6PDI (Supporting Information) and found that the relative intensities of the 0–0 and 0–1 vibration bands of 6PDI are temperature and concentration independent. This excludes the possibility of intermolecular aggregation of 6PDI in solution, and the difference between the absorption spectra of 2PDI and 6PDI must be the result of intramolecular interactions.

The optimized structures, obtained with the AM1 method in the Gaussian03 software package, of these two compounds are shown in Figure 2, and the related parameters are labeled. The center-to-center distances between the neighboring PDI subunits in 2PDI are the same as those in 6PDI, but the dihedral angle (α) between the PDI plane and the central phenyl ring in 2PDI is significantly smaller than that in 6PDI (25.66 vs 35.77°). As a result of the larger dihedral angle between the

© 2013 Wiley-VCH Verlag GmbH & Co. KGaA, Weinheim

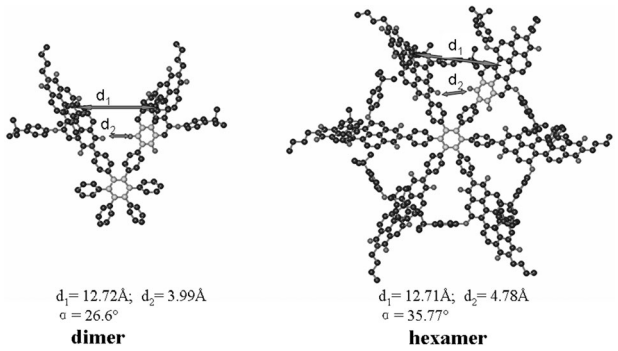

Figure 2. Minimized structures of 2PDI and 6PDI. d_1 = center-to-center distance, d_2 = edge-to-edge distance between neighboring PDI subunits, α = dihedral angle between the two six-member rings highlighted in light gray.

PDI plane and the central phenyl ring in 6PDI, the relative orientation of the neighboring PDI subunits is more of a "face-to-face" stacking mode. Moreover, the PDI subunits in 2PDI can rotate freely along the molecular long axis, but in 6PDI, the rotation of the PDI subunits along the molecular long axis is blocked due to steric hindrance of the two neighboring subunits. We suggest that the larger dihedral angle and the blocked free rotation of the PDI subunits in 6PDI are responsible for the different absorption spectra of 6PDI and 2PDI.

The normalized fluorescence spectra of the monomer, 2PDI, and 6PDI are shown in Figure 3. The maximum emission peak for 2PDI and 6PDI is close to that of the monomer, which suggests that the emission is dominated by the fluorescence of the monomeric PDI. However, in the emission band of both 2PDI and 6PDI, a tail extending to longer wavelengths can be identified. This tail is more significant in the spectrum of 6PDI than in the spectrum of 2PDI, which corresponds well with the stronger interactions among the PDI subunits in 6PDI, as revealed by the absorption spectra. The emission tail in the long-wavelength region can be assigned to "excimer-like" states due to face-to-face interactions.[43] The fluorescence quantum yields of these three compounds were also measured, and the results are summarized in Table 1.

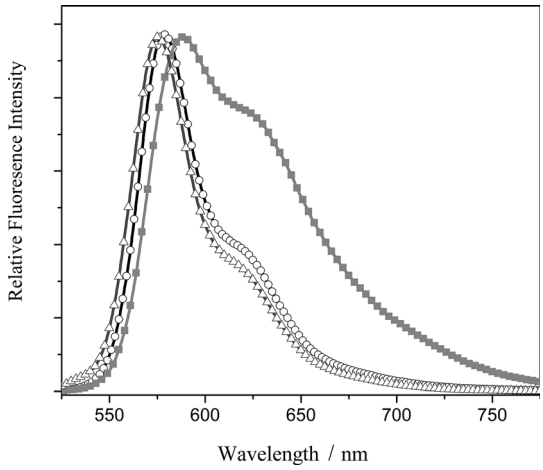

Figure 3. Normalized fluorescence spectra of 6PDI (□), 2PDI (○), and monomer (△) in CH_2Cl_2 (1.0×10^{-6} mol L^{-1}).

With the monomer as the standard, the fluorescence quantum yield of 2PDI and 6PDI was found to be 0.42 and 0.08, respectively, and these are both much smaller than the quantum yield of the monomer. This result suggests that there are interactions between or among the PDI subunits in 2PDI and 6PDI. The interactions induce some nonradiative decay in the excited states and thus reduce the fluorescence quantum yields significantly. This phenomenon has also been found for other PDI aggregates.[43,44] Moreover, the fluorescence quantum yield of 6PDI is smaller than that of 2PDI, which indicates that interactions among the PDI subunits in 6PDI are stronger than those in 2PDI. This is consistent with the results obtained from the absorption spectra and can be explained as the aforementioned difference in the relative orientation of the PDI subunits in the minimized structures of 2PDI and 6PDI.

The fluorescence lifetimes of these three compounds were also measured by time-correlated single photon counting (TCSPC) at 600 nm. The lifetime of the monomer is 4.5 ns, which is similar to literature results.[44] However, the fluorescence of 6PDI and 2PDI show biexponential decay, and thus, two fluorescence lifetimes can be measured. The short one, with a lifetime of 4.3 ns for 2PDI and 4.1 ns for 6PDI, can be ascribed to monomeric fluorescence. The long fluorescence lifetime component might be attributed to the emission of "excimer-like" states. "Excimer-like" states of PDIs always show lifetimes of fluorescence that are longer than those of the monomer. The longest lifetime reported so far is 28 ns, which was presented by a cyclic PDI dimer with a relatively rigid structure.[44] However, the "excimer-like" state of a PDI dimer with a relatively flexible structure was also reported to show a fluorescence lifetime of around 18 ns.[43] Therefore, the fluorescence lifetime of PDI "excimer-like" states varies dramatically between compounds with different structures. The rigid structure with the strictly face-to-face stacked model will lead to a longer fluorescence lifetime for the "excimer-like" states of PDI, and weak interactions or a flexible PDI dimer may cause a relatively short fluorescence lifetime for the "excimer-like" states. The lifetimes of the "excimer-like" states in 6PDI and 2PDI are relatively short, which suggests that the interactions between or among the PDI subunits in these compounds are relatively weak.[43]

Electrochemical Properties

Weak ground-state interactions between/among the PDI subunits were also revealed by electrochemical experiments. Differential pulse voltammetry was performed for these three compounds, and the results are shown in Figure 4 and the experimental data are summarized in Table 2. The electrochemical behavior of these three compounds is very similar. One oxidation peak appears at a relatively high positive voltage and two reduction peaks appear in the negative region. However, tiny differences can still be identified among these three compounds. The first reduction occurs at −0.61 V for the monomer, but this peak moves to −0.63 and −0.65 V for 2PDI and

© 2013 Wiley-VCH Verlag GmbH & Co. KGaA, Weinheim

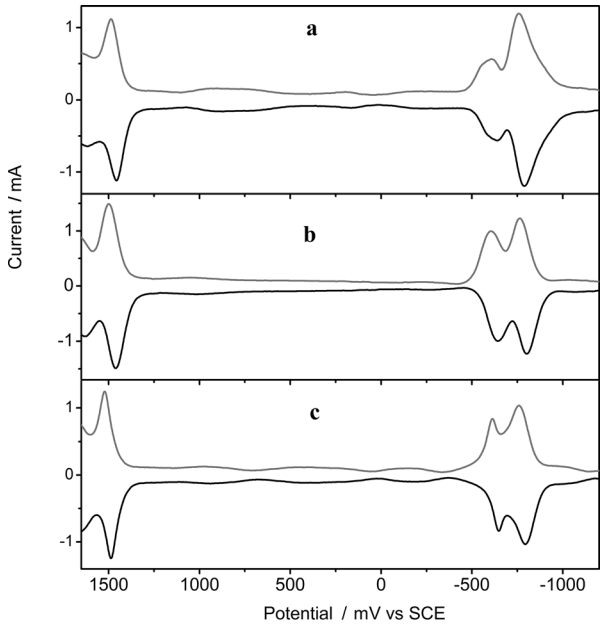

Figure 4. Differential pulse voltammetry of a) the monomer, b) 2PDI, and c) 6PDI in CH_2Cl_2 containing 0.1 M $[Bu_4N^+][ClO_4^-]$.

Table 2. Half-wave redox potentials [V vs SCE] of the monomer, 2PDI, and 6PDI in CH_2Cl_2 containing 0.1 M $[Bu_4N][ClO_4]$.

Compound	Oxd_1 [V]	Red_1 [V]	Red_2 [V]	$\Delta E^0_{1/2}$ [a] [V]
monomer	1.48	−0.61	−0.79	2.09
2PDI	1.48	−0.63	−0.79	2.11
6PDI	1.50	−0.65	−0.78	2.15

[a] $\Delta E^0_{1/2} = O_{oxd_1} - R_{red_1}$

6PDI, respectively. This negative shift in the first reduction potential implies that it is more difficult to reduce 2PDI and 6PDI than the monomer. Because the reduction process is closely related to the energy levels of the LUMO, the more negative first reduction potential of 6PDI and 2PDI indicates that their LUMOs lie at a higher energy level. The shift in the first reduction potential suggests the presence of interactions between/among the PDI subunits in 6PDI and 2PDI, but the significance of these interactions is small.

Ultrafast Transient Anisotropy Decay Dynamics

To further explore the relaxation dynamics of the excited-state interactions, we performed femtosecond transient absorption anisotropy (TAA) experiments on these three compounds. Anisotropy decay implies a dependence on the relative orientations of the pump and probe polarizations, which is caused by reorientation of excitonically coupled transition dipole moments or by differently oriented transition dipole moments if excitation of an energy hopping process (i.e. EET) exists.[14,56] Studies on anisotropy depolarization of natural light-harvesting systems (i.e. LH1 and LH2) that have circular arrangements with constant interactions between the neighboring chlorophyll units have been well documented.[62–65]

In addition to the TAA experiments, femtosecond transient absorption (TA) spectra were recorded for the three compounds, and the results are shown in the Supporting Information. The TA spectra of the three compounds are similar and feature three groups of peaks. The first group of peaks results from ground-state bleaching (GSB), and they present as two negative peaks around 510 and 550 nm. The second group of signals results from excited-state absorption (ESA), and they appear around 710 nm as broad positive peaks. This ESA band may actually extend into the lower wavelength region, but this cannot be discerned because of strong overlap with the more-pronounced GSB band. Besides the GSB and ESA bands, a stimulated emission (SE) band can be found in the 550–650 nm region in the TA spectra of the monomer and 2PDI. The SE band is not found in the TA spectrum of 6PDI because the relatively strong interactions between the PDI subunits enhance the nonradiative decay pathway for the singlet excited states of the PDIs. This corresponds well with the results obtained from the stationary absorption and fluorescence spectra.

Figure 5 presents the time dependence of the anisotropy (r) of the monomer, 2PDI, and 6PDI probed at 710 nm, in which the ESA signal dominates the absorption difference spectra, followed by the 400 nm excitation. The fitting results are summarized in Table 3. Notably, after the initial 10 ps, the anisotropy is nearly constant for all three compounds. The anisotropy dynamics of 2PDI and 6PDI are significantly different from those of the monomer. Upon photoexcitation of the S_2 state (400 nm), all three compounds showed ultrafast anisotropy decay from a value near 0.4 to a negative value. This is reason-

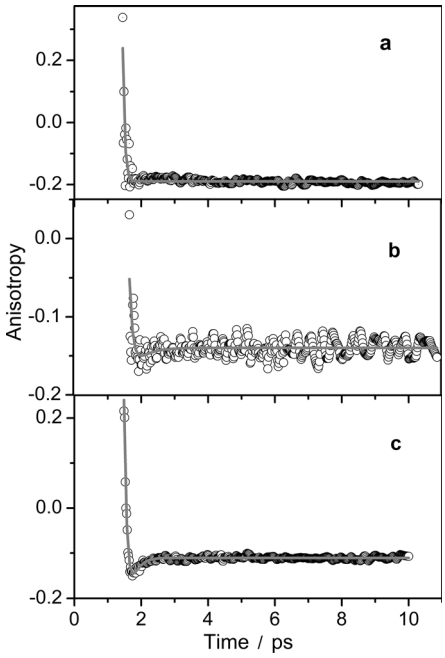

Figure 5. Transient absorption anisotropy decay profiles of a) the monomer, b) 2PDI, and c) 6PDI in CH_2Cl_2.

© 2013 Wiley-VCH Verlag GmbH & Co. KGaA, Weinheim

Table 3. Fitting results of the anisotropic decay at 710 nm for the monomer, 2PDI, and 6PDI.[a]

Compound	τ_1 [fs]	τ_2 [fs]	τ_3[b] [ps]
monomer	97	–	>10
2PDI	100	371	>10
6PDI	100	168	>10

[a] The value of χ^2 for each fitting was in the range of 1.05–1.24. [b] Long component in the TAA decay, which was longer than the time window of the experiment.

able for PDI derivatives, for the dipole moment of the S_0–S_2 electronic transition is perpendicular to that of the S_0–S_1 transition.[66,67] By fitting the decay profile of the monomer with a biexponential function, two time constants were obtained. The short one (172 fs) can be assigned to the relaxation from S_2 to S_1, in which the long lifetime component (beyond the experimental time window, >10 ps) is due to the rotation diffusion of the molecules. Three time constants were obtained from the best fits of the profiles of the TAA spectra of 2PDI and 6PDI. The shortest (100 fs for both 2PDI and 6PDI) and longest (>10 ps) components are similar to those of the monomer and, therefore, can be assigned to S_2 to S_1 internal conversion and rotation diffusion, respectively. Another fast component (371 fs for 2PDI and 168 fs for 6PDI) was found in the TAA decay of 2PDI and 6PDI. On the basis of previous observations of the different absorption spectra, a delocalized exciton state is formed in branched 2PDI and 6PDI, and it is reasonable to attribute this second fast component in 2PDI and 6PDI to excitation delocalization between/among the different PDI branches.[68] From the fitting results, delocalization of the excited states in 6PDI (168 fs) is faster than that in 2PDI (371 fs), which supports the idea that the intramolecular interactions in 6PDI are stronger than those in 2PDI. This behavior is also seen in photosynthetic light-harvesting antenna pigment systems.[69]

3. Conclusions

In summary, a PDI dimer and a wheel-like hexamer linked by the same hexaphenylbenzene group were prepared. Due to greater steric hindrance in 6PDI caused by the two neighboring PDI subunits, rotation of the PDI subunits along the molecular long axis is blocked, whereas the PDI subunits in 2PDI can rotate freely. Thus, interactions among the PDI subunits in 6PDI are relatively stronger than those in 2PDI, as revealed by stationary absorption and fluorescence spectra. Quick and efficient excitation delocalization between/among the PDI subunits was found in both 6PDI and 2PDI. Excitation energy delocalization in 6PDI is faster than that in 2PDI, which can be ascribed to stronger ground-state interactions among the PDI subunits in 6PDI. This result demonstrates successfully that the photophysical properties of 2PDI and 6PDI are significantly different from each other even though they have similar molecular structures. The subtle difference in the flexibility of the molecules may cause a dramatic change in the interactions between the PDI subunits and finally affect the excitation energy delocalization process.

Experimental Section

General Information

^{1}H NMR spectra were recorded with a Bruker 300 or 400 MHz NMR spectrometer. Chemical shifts are reported relative to tetramethylsilane as an internal standard. MALDI-TOF mass spectra were recorded with a Bruker/ultra flex instrument. Absorption spectra were measured with a Hitachi U-4100 spectrophotometer. Fluorescence spectra and fluorescence lifetimes were measured with an ISS K2 system. The fluorescence lifetimes were measured with a phase modulation model with a scattering sample as standard. Electrochemical measurements were performed with a BAS CV-50W voltammetric analyzer. The cell comprised inlets for a glassy carbon disk working electrode that was 2.0 mm in diameter and a silver-wire counterelectrode. The reference electrode was Ag/Ag^+, which was connected to the solution by a Luggin capillary, the tip of which was placed close to the working electrode. It was corrected for junction potentials by referencing internally to the ferrocenium/ferrocene (Fc^+/Fc) couple [$E_{1/2}$ (Fc^+/Fc) = 501 mV vs SCE]. Typically, a 0.1 mol L^{-1} solution of $[Bu_4N][ClO_4]$ in CH_2Cl_2 containing 0.5 mmol L^{-1} of sample was purged with nitrogen for 15 min, and then the voltammograms were recorded at ambient temperature. The scan rate was 10 mV s^{-1} for differential pulse voltammetry. The transient absorption spectra and anisotropic decay were measured by using a homemade femtosecond broadband pump–probe setup. Experimental details can be found in the Supporting Information.

Synthesis and Characterization

Compound **1**: A 100 mL, three-necked flask was charged with *N*-butyl-1,7-di(4-*tert*-butyl)phenoxyl-perylene-3,4-dicarboxylic imide-9,10-dicarboxylic anhydride (148 mg, 0.2 mmol), bis(4-aminophenyl)ethyne (20 mg, 0.1 mmol), toluene (20 mL), and imidazole (1.5 g). The mixture was heated to 116 °C and kept at this temperature for about 10 h. The progress of the reaction was monitored by thin-layer chromatography (TLC). Upon complete consumption of the reactant as revealed by TLC, the reaction mixture was evaporated to dryness under reduced pressure. The residue was dissolved in chloroform and washed with water repeatedly to remove imidazole. The organic layer was dried with anhydrous magnesium sulfate overnight, and the solvent was then evaporated. The residue was purified by column chromatography on silica gel (chloroform/methanol = 98:2). Compound **1** was collected as a red solid (39.8 mg, 24%). ^{1}H NMR (300 MHz, $CDCl_3$): δ = 9.11–9.25 (d, 4H), 8.23–8.42 (d, 4H), 8.11 (d, 4H), 7.66–7.68 (d, 4H), 7.44–7.48 (t, 4H), 7.36 (m, 8H), 6.84–6.94 (m, 8H), 3.2 (t, 4H), 1.59–1.64 (t, 4H), 1.32–1.34 (m, 40H), 0.98 ppm (m, 6H). MS (MALDI-TOF): *m/z*: 1660.17 $[M]^+$ ($C_{110}H_{90}N_4O_{12}$ calcd 1659.96). Elemental analysis calcd (%) for $C_{110}H_{90}N_4O_{12}$ (1659.66): C 79.59, H 5.47, N 3.38; found: C 79.32, H 5.36, N 3.36.

2PDI: A 100 mL, three-necked flask was charged with **1** (166 mg, 0.1 mmol) and tetraphenylcyclopentadienone (38 mg, 0.1 mmol); diphenyl ether (100 mL) was then added. The reaction mixture was heated at reflux for 12 h, and the reaction mixture was then cooled to room temperature and poured into methanol (100 mL). The solid was separated by filtration and dried at room temperature. The product was purified by column chromatography on silica gel (dichloromethane). 2PDI was collected as a red solid

© 2013 Wiley-VCH Verlag GmbH & Co. KGaA, Weinheim

(10 mg, 5%). ^{1}H NMR (300 MHz, $CDCl_3$): $\delta = 9.53$ (d, 4H), 8.51–8.53 (d, 2H), 8.42–8.44 (d, 2H), 8.31 (s, 2H), 8.21 (s, 2H), 7.39–7.41 (d, 4H), 7.34–7.36 (d, 4H), 7.02–7.04 (d, 4H), 6.97–6.99 (d, 4H), 6.86–6.92 (m, 28H), 3.24 (t, 4H), 1.57–1.62 (t, 4H), 1.31–1.34 (m, 40H), 0.87 ppm (m, 6H). MS (MALDI-TOF): *m/z*: 2015.96 $[M]^+$ ($C_{138}H_{110}N_4O_{12}$ calcd 2016.44). Elemental analysis (%) calcd for $C_{138}H_{110}N_4O_{12}$ (2016.44): C 82.2, H 5.5, N 2.78; found: C 82.17, H 5.47, N 2.58.

6PDI: Under an atmosphere of nitrogen, a three-necked flask was charged with **1** (166 mg, 0.1 mmol), dry 1,4-dioxane (20 mL), and $Co_2(CO)_8$ (10 mg). The reaction mixture was heated at reflux for 12h. The solvent was then evaporated to dryness under reduced pressure. The residue was purified by column chromatography on silica gel (dichloromethane), and 6PDI was collected as a dark red solid (5.94 mg, 4%). ^{1}H NMR (300 MHz, $CDCl_3$): $\delta = 9.28$–9.42 (br, 12H), 8.40–8.60 (br, 12H), 8.12–8.35 (br, 12H), 7.60–7.80 (m, 24H), 6.89–7.01 (m, 24H), 6.72–6.86 (m, 24H), 4.08–4.13 (d, 12H), 1.56 (t, 12H), 1.26–1.35 (m, 120H), 0.87–0.97 ppm (m, 18H). MS (MALDI-TOF): *m/z*: 4980.7 $[M]^+$ ($C_{330}H_{270}N_{12}O_{36}$ calcd 4979.89). Elemental analysis (%) calcd for $C_{330}H_{270}N_{12}O_{36}$ (4979.89): C 79.59, H 5.47, N 3.38; found: C 79.47, H 5.42, N 3.27.

Acknowledgements

We thank the Natural Science Foundation of China (Grant Nos. 21073112, 21173136, and 91233108), the National Basic Research Program of China (973 Program: 2012CB93280), and the Natural Science Foundation of Shandong Province (ZR2010EZ007) for financial support. Many thanks to Prof. Andong Xia and Dr. Yingying Wang from the Institute of Chemistry, Chinese Academy of Sciences for the transient absorption measurements and ultrafast transient anisotropy decay experiments.

Keywords: dyes/pigments · excitation delocalization · fluorescence · intramolecular interactions · UV/Vis spectroscopy

[1] G. McDermott, S. M. Prince, A. A. Freer, A. M. Hawthornthwaite-Lawless, M. Z. Papiz, R. J. Cogdell, N. W. Isaacs, *Nature* **1995**, *374*, 517–521.
[2] J. Koepke, X. Hu, C. Muenke, K. Schulten, H. Michel, *Structure* **1996**, *4*, 581–597.
[3] A. W. Roszak, T. D. Howard, J. Southall, A. T. Gardiner, C. J. Law, N. W. Isaacs, R. J. Cogdell, *Science* **2003**, *302*, 1969–1972.
[4] S. Anderson, H. L. Anderson, J. K. M. Sanders, *Acc. Chem. Res.* **1993**, *26*, 469–475.
[5] B. Rybtchinski, L. S. Sinks, M. R. Wasielewski, *J. Am. Chem. Soc.* **2004**, *126*, 12268–12269.
[6] D. Gust, T. A. Moore, A. L. Moore, *Acc. Chem. Res.* **2001**, *34*, 40–48.
[7] D. Gust, T. A. Moore, A. L. Moore, *Acc. Chem. Res.* **2009**, *42*, 1890–1898 and references cited therein.
[8] M. A. Fox, *Acc. Chem. Res.* **2012**, *45*, 1875–1886.
[9] M. R. Wasielewski, *Acc. Chem. Res.* **2009**, *42*, 1910–1921.
[10] Y. Nakamura, N. Aratani, A. Osuka, *Chem. Soc. Rev.* **2007**, *36*, 831–845.
[11] R. F. Kelley, R. H. Goldsmith, M. R. Wasielewski, *J. Am. Chem. Soc.* **2007**, *129*, 6384–6385.
[12] Y. Kubo, Y. Kitada, R. Wakabayashi, T. Kishida, M. Ayabe, K. Kaneko, M. Takeuchi, S. Shinkai, *Angew. Chem.* **2006**, *118*, 1578–1583; *Angew. Chem. Int. Ed.* **2006**, *45*, 1548–1553.
[13] I. W. Hwang, M. Park, T. K. Ahn, Z. S. Yoon, D. M. Ko, D. Kim, F. Ito, Y. Ishibashi, S. R. Khan, Y. Nagasawa, H. Miyasaka, C. Ikeda, R. Takahashi, K. Ogawa, A. Satake, Y. Kobuke, *Chem. Eur. J.* **2005**, *11*, 3753–3761.
[14] Y. Nakamura, I. W. Hwang, N. Aratani, T. K. Ahn, D. M. Ko, A. Takagi, T. Kawai, T. Matsumoto, D. Kim, A. Osuka, *J. Am. Chem. Soc.* **2005**, *127*, 236–246.
[15] M. Hoffmann, J. Karnbratt, M. H. Chang, L. M. Herz, B. Albinsson, H. L. Anderson, *Angew. Chem.* **2008**, *120*, 5071–5074; *Angew. Chem. Int. Ed.* **2008**, *47*, 4993–4996.
[16] M. Hoffmann, C. J. Wilson, B. Odell, H. L. Anderson, *Angew. Chem.* **2007**, *119*, 3183–3186; *Angew. Chem. Int. Ed.* **2007**, *46*, 3122–3125.
[17] O. Mongin, A. Schuwey, M. A. Vallot, A. Gossauer, *Tetrahedron Lett.* **1999**, *40*, 8347–8350.
[18] J. Z. Li, A. Ambroise, S. I. Yang, J. R. Diers, J. Seth, C. R. Wack, D. F. Bocian, D. Holten, J. S. Lindsey, *J. Am. Chem. Soc.* **1999**, *121*, 8927–8940.
[19] R. W. Wagner, J. Seth, S. I. Yang, D. Kim, D. F. Bocian, D. Holten, J. S. Lindsey, *J. Org. Chem.* **1998**, *63*, 5042–5049.
[20] N. Aratani, A. Osuka, *Chem. Commun.* **2008**, 4067–4069.
[21] A. Vidal-Ferran, Z. Clyde-Watson, N. Bampos, J. K. M. Sanders, *J. Org. Chem.* **1997**, *62*, 240–241.
[22] S. Rucareanu, O. Mongin, A. Schuwey, N. Hoyler, A. Gossauer, W. Amrein, H.-U. Hediger, *J. Org. Chem.* **2001**, *66*, 4973–4988.
[23] R. W. Wagner, J. S. Lindsey, J. Seth, V. Palaniappan, D. F. Bocian, *J. Am. Chem. Soc.* **1996**, *118*, 3996–3997.
[24] H. A. M. Biemans, A. E. Rowan, A. Verhoeven, P. Vanoppen, L. Latterini, J. Foekema, A. P. H. J. Schenning, E. W. Meijer, F. C. de Schryver, R. J. M. Nolte, *J. Am. Chem. Soc.* **1998**, *120*, 11054–11060.
[25] Y. Terazono, G. Kodis, P. A. Liddell, V. Garg, T. A. Moore, A. L. Moore, D. Gust, *J. Phys. Chem. B* **2009**, *113*, 7147–7155.
[26] G. Kodis, Y. Terazono, P. A. Liddell, J. Andréasson, V. Garg, M. Hambourger, T. A. Moore, A. L. Moore, D. Gust, *J. Am. Chem. Soc.* **2006**, *128*, 1818–1827.
[27] Z. Tomović, J. V. Dongen, S. J. George, H. Xu, W. Pisula, P. Leclère, M. M. J. Smulders, S. D. Feyter, E. W. Meijer, A. P. H. J. Schenning, *J. Am. Chem. Soc.* **2007**, *129*, 16190–16196.
[28] L. Flamigni, B. Ventura, C. C. You, C. Hippius, F. Würthner, *J. Phys. Chem. C* **2007**, *111*, 622–630.
[29] B. K. An, J. Gierschner, S. Y. Park, *Acc. Chem. Res.* **2012**, *45*, 544–554.
[30] F. J. M. Hoeben, I. O. Shklyarevskiy, M. J. Pouderoijen, H. Engelkamp, A. P. H. J. Schenning, P. C. M. Christianen, J. C. Maan, E. W. Meijer, *Angew. Chem.* **2006**, *118*, 1254–1258; *Angew. Chem. Int. Ed.* **2006**, *45*, 1232–1236.
[31] C. Hippius, T. H. M. Stokkum, M. Gsänger, M. M. Groeneveld, R. M. Williams, F. Würthner, *J. Phys. Chem. C* **2008**, *112*, 2476–2486.
[32] M. J. Ahrens, L. E. Sinks, B. Rybtchinski, W. Liu, B. A. Jones, J. M. Giaimo, A. V. Gusev, A. J. Goshe, D. M. Tiede, M. R. Wasielewski, *J. Am. Chem. Soc.* **2004**, *126*, 8284–8294.
[33] A. Sautter, B. Kükrer Kaletaş, D. G. Schmid, R. Dobrawa, M. Zimine, G. Jung, I. H. M. van Stokkum, L. De Cola, R. M. Williams, F. Würthner, *J. Am. Chem. Soc.* **2005**, *127*, 6719–6729.
[34] H. Langhals, *Helv. Chim. Acta* **2005**, *88*, 1309–1343 and references cited therein.
[35] X. Y. Li, L. E. Sinks, B. Rybtchinski, M. R. Wasielewski, *J. Am. Chem. Soc.* **2004**, *126*, 10810–10811.
[36] C. Hippius, I. H. M. van Stokkum, E. Zangrando, R. M. Williams, F. Würthner, *J. Phys. Chem. C* **2007**, *111*, 13988–13996.
[37] C. Hippius, F. Schlosser, M. O. Vysotsky, V. Böhmer, F. Würthner, *J. Am. Chem. Soc.* **2006**, *128*, 3870–3871.
[38] H. Langhals, M. Rauscher, J. Strübe, D. Kuck, *J. Org. Chem.* **2008**, *73*, 1113–1116.
[39] F. Würthner, *Chem. Commun.* **2004**, 1564–1579.
[40] C. T. Zhao, Y. X. Zhang, R. J. Li, X. Y. Li, J. Z. Jiang, *J. Org. Chem.* **2007**, *72*, 2402–2410.
[41] T. van der Boom, R. T. Hayes, Y. Y. Zhao, P. J. Bushard, E. A. Weiss, M. R. Wasielewski, *J. Am. Chem. Soc.* **2002**, *124*, 9582–9590.
[42] H. Langhals, R. Ismael, *Eur. J. Org. Chem.* **1998**, 1915–1917.
[43] Y. F. Wang, Y. L. Chen, R. J. Li, S. Q. Wang, W. Su, P. Ma, M. R. Wasielewski, X. Y. Li, J. Z. Jiang, *Langmuir* **2007**, *23*, 5836–5842.
[44] J. Q. Feng, Y. X. Zhang, C. T. Zhao, R. J. Li, W. Xu, X. Y. Li, J. Z. Jiang, *Chem. Eur. J.* **2008**, *14*, 7000–7010.
[45] J. M. Giaimo, A. V. Gusev, M. R. Wasielewski, *J. Am. Chem. Soc.* **2002**, *124*, 8530–8531.
[46] J. M. Giaimo, J. V. Lockard, L. E. Sinks, A. M. Scott, T. M. Wilson, M. R. Wasielewski, *J. Phys. Chem. A* **2008**, *112*, 2322–2330.
[47] H. Yoo, J. Yang, A. Yousef, M. R. Wasielewski, D. Kim, *J. Am. Chem. Soc.* **2010**, *132*, 3939–3944.

© 2013 Wiley-VCH Verlag GmbH & Co. KGaA, Weinheim

[48] T. Ishi-i, K. Murakami, Y. Imai, S. Mataka, *J. Org. Chem.* **2006**, *71*, 5752 – 5760.
[49] H. Langhals, J. Gold, *J. Prakt. Chem.* **1996**, *338*, 654 – 659.
[50] J. Wu, J. Qu, N. Tchebotareva, K. Müllen, *Tetrahedron Lett.* **2005**, *46*, 1565 – 1568.
[51] L. F. Dössel, V. Kamm, I. A. Howard, F. Laquai, W. Pisula, X. Feng, C. Li, M. Takase, T. Kudernac, S. De Feyter, K. Müllen, *J. Am. Chem. Soc.* **2012**, *134*, 5876 – 5886.
[52] H. Langhals, A. J. Esterbauer, A. Walter, E. Riedle, I. Pugliesi, *J. Am. Chem. Soc.* **2010**, *132*, 16777 – 16782.
[53] Y. N. Du, L. L. Jiang, J. Zhou, G. J. Qi, X. Y. Li, *Org. Lett.* **2012**, *14*, 3052 – 3055.
[54] H. Langhals, M. Speckbacher, *Eur. J. Org. Chem.* **2001**, 2481 – 2486.
[55] L. Xue, H. X. Wu, Y. Shi, H. Y. Liu, Y. L. Chen, X. Y. Li, *Soft Matter* **2011**, *7*, 6213 – 6221.
[56] H. S. Cho, H. Rhee, J. K. Song, C. K. Min, M. Takase, N. Aratani, S. Cho, A. Osuka, T. Joo, D. Kim, *J. Am. Chem. Soc.* **2003**, *125*, 5849 – 5860.
[57] V. J. Chebny, D. Dhar, S. V. Lindeman, R. Rathore, *Org. Lett.* **2006**, *8*, 5041 – 5044.
[58] D. Nishimura, T. Oshikiri, Y. Takashima, A. Hashidzume, H. Yamaguchi, A. Harada, *J. Org. Chem.* **2008**, *73*, 2496 – 2502.
[59] P. M. Kazmaier, R. Hoffmann, *J. Am. Chem. Soc.* **1994**, *116*, 9684 – 9691.
[60] W. Wang, L.-S. Li, G. Helms, H.-H. Zhou, A. D. Q. Li, *J. Am. Chem. Soc.* **2003**, *125*, 1120 – 1121.
[61] W. Wang, L. Q. Wang, J. Palmer, G. Exarhos, A. D. Q. Li, *J. Am. Chem. Soc.* **2006**, *128*, 11150 – 11159.
[62] S. E. Bradforth, R. Jimenez, F. van Mourik, R. van Grondelle, G. R. Fleming, *J. Phys. Chem.* **1995**, *99*, 16179 – 16191.
[63] G. Trinkunas, J. L. Herek, T. Polívka, V. Sundström, T. Pullerits, *Phys. Rev. Lett.* **2001**, *86*, 4167 – 4170.
[64] B. Brüggemann, V. May, *J. Chem. Phys.* **2004**, *120*, 2325 – 2336.
[65] B. Brüggemann, J. L. Herek, V. Sundström, T. Pullerits, V. May, *J. Phys. Chem. B* **2001**, *105*, 11391 – 11394.
[66] M. D. Barkley, A. A. Kowalczyk, L. Brand, *J. Chem. Phys.* **1981**, *75*, 3581 – 3593.
[67] X. M. Guo, Y. Wan, A. D. Xia, S. F. Wang, J. Y. Liu, H. K. Li, *Chin. Phys. B* **2009**, *18*, 142 – 148.
[68] F. Zhao, X. Zheng, J. Zhang, H. Wang, Z. Yu, J. Zhao, L. Jiang, *J. Photochem. Photobiol. B* **1998**, *45*, 144 – 149.
[69] T. Goodson III, *Acc. Chem. Res.* **2005**, *38*, 99 – 107.

Received: June 26, 2013
Published online on July 24, 2013

© 2013 Wiley-VCH Verlag GmbH & Co. KGaA, Weinheim